

SAR-NAS: Skeleton-based Action Recognition via Neural Architecture Searching

Haoyuan Zhang, Yonghong Hou, *Member, IEEE*, Pichao Wang, *Member, IEEE*, Zihui Guo, Wanqing Li, *Senior Member, IEEE*,

Abstract—This paper presents a study of automatic design of neural network architectures for skeleton-based action recognition. Specifically, we encode a skeleton-based action instance into a tensor and carefully define a set of operations to build two types of network cells: normal cells and reduction cells. The recently developed DARTS (Differentiable Architecture Search) is adopted to search for an effective network architecture that is built upon the two types of cells. All operations are 2D based in order to reduce the overall computation and search space. Experiments on the challenging NTU RGB+D and Kinetics datasets have verified that most of the networks developed to date for skeleton-based action recognition are likely not compact and efficient. The proposed method provides an approach to search for such a compact network that is able to achieve comparative or even better performance than the state-of-the-art methods.

Index Terms—Neural Architecture Search, Action Recognition, Skeleton.

I. INTRODUCTION

AS an active and challenging research topic in computer vision, human action recognition has many potential applications such as human computer interaction, autonomous retail shops, autonomous driving and somatic games [1], [2]. In general, human action can be recognized from multiple modalities, such as RGB, optical flows, and skeletons. In the past decades, researcher mainly focused on RGB-based action recognition. With the advent of deep learning, neural networks are widely employed to learn robust feature representations [3]–[8]. Although the RGB-based methods do well in the extraction of spatial feature from videos, motion between video frames are not well captured [9], as a result optical flow is used for temporal complementation [10], [11]. Driven by the advances in skeleton estimation from RGB and depth modality, skeleton data is becoming a common modality in action recognition [12]–[18]. On the one hand, skeleton data is robust against the complex conditions such as occlusion, self-occlusion and variations of the subjects and viewpoints. On the other hand, skeleton data can be easily encoded into images so that conventional convolutional neural networks (CNN) [19]–[22] and recurrent neural networks (RNN) [23]–[27] can be

employed. To date, many deep neural networks have been developed for skeleton-based action recognition [19], [28]–[30]. However, design and tuning of such networks requires much time and human efforts. Moreover, the network architecture becomes more and more complicated in order to effectively exploit spatial-temporal information, hence more expensive to design and train [1]. Neural architecture search (NAS) has recently emerged as an effective approach to automating the design of a deep neural network. The key idea of NAS is to build a search space consisting of as many feasible network architectures as possible, then to explore the search space with an efficient algorithm and find out an optimal architecture for a given task under some constraints [31]. NAS has been successfully used to discover neural architectures for tasks such as image classification [32], semantic image segmentation [33] and object detection tasks [34]. However, little work has been reported on discovering a suitable architecture for skeleton-based action recognition.

This paper targets to fill this gap by exploiting NAS for skeleton-based action recognition. However, finding a feasible architecture in the large search space is usually time-consuming. The recent one-shot approach successfully reduces the cost of architecture discovery by an order of magnitudes compared with previous methods [35], [36]. DARTS (Differentiable Architecture Search) [35] offers an alternative efficient method by relaxing the categorical choice of a particular operation in NAS to a softmax over all possible operations to make the search space continuous so that classic gradient-based optimization can be used. To take advantages of DARTS [35], we propose to adopt it to construct a compact CNN architecture for skeleton-based action recognition. An action instance is uniformly sampled into $T \times N \times 3$ data representation as input to the network, where T , N are the number of frames and number of joints respectively and the 3D coordinates are treated as three channels. In order to construct an effective compact CNN architecture and also keep the search space of DARTS small, a set of operators is carefully chosen. First, the kernel sizes of all operators are relatively small and dilated convolution is used to increase the reception filed with less number of parameters. Second, squeeze-and-excitation module [37] is chosen as an operator to capture the importance of each channel (i.e. motion in the Euclidean planes) to provide a channel-wise attention mechanism. Third, all operators are 2D-based for its low computational cost and high searching efficiency so that direct search on a large scale dataset without proxy is achieved. In addition, the 2D convolutional operations work along the tem-

This paper was supported by National Natural Science Foundation of China (61571325) in Tianjin, China. (Corresponding author: Pichao Wang)

H. Zhang, Y. Hou and Z. Guo are with the School of Electronic Information Engineering, Tianjing University, Tianjin, China. (e-mail: zhy0860@tju.edu.cn; houroy@tju.edu.cn; gzihui@tju.edu.cn).

P. Wang is with the Alibaba DAMO Academy, Bellevue, USA. (e-mail: pichaowang@gmail.com).

W. Li is with the Advanced Multimedia Research Lab, University of Wollongong, Wollongong, Australia. (e-mail: wanqing@uow.edu.au).

poral domain forming an effective Temporal 2D Convolutional Network (TCN). Through the multiple stages of convolution and pooling operations, local temporal information is gradually encoded into global one. The efficacy of these design strategies have been verified on two large scale datasets including NTU RGB+D [38] and Kinetics [39].

II. PROPOSED METHOD

Fig. 1 shows the modularized network architecture C to be searched. Follow the idea in DARTS [35], computation cells as the building blocks are defined and searched. The learned cells are then stacked together to form a complete network. Noted that a relative shallow network architecture is adopted since the limitation of GPU memory though the idea presented in this paper can be easily extended to a deep network.

There are two types of cells, normal cells and reduction cells. The normal cells employ operations with stride 1 and reduction cells employ operations with stride 2 in order to halve the spatial dimension of the input. Each cell consists of several nodes and each node is a specific tensor-like feature map. A directed edge of two nodes works as an operation sampled from a set O of candidate operators to transform one node to another. There are three types of nodes in a cell: input node, intermediate node and output node. Output tensors from previous cells are taken as input nodes, then through applying sampled operations to input nodes the intermediate nodes are generated, finally all intermediate nodes are concatenated to get the output node of current cell. Each cell is assumed to have two input nodes, four intermediate nodes and one output node, where 14 connections exit.

As one of the most important elements in neural architecture search (NAS), search space is determined by the operators that may constitute an architecture and should be minimized for efficacy. Table I lists the eight candidate operators that are carefully chosen for O . First, use of 3×3 dilated convolution (with dilation rate 2) and separable convolution as those in DARTS [35], removal of two 5×5 convolution operators, and inclusion of a normal 3×3 operator aim to reduce the number of parameters while keeping the same possible receptive field. Second, to use the squeeze-and-excitation module as a candidate operator aims to provide a channel-wise attention mechanism to select important channels. Third, as in DARTS [35], the max and average pooling operators provide two different ways to aggregate features, and skip-connect avoids vanishing gradient in deep architectures. Besides, for the sake of computational and searching efficiency, all operators are 2D based. For normal cells, all operations are of stride one and the convolved feature maps are padded to preserve their spatial resolution. For reduction cells located at the $\frac{1}{3}$ and $\frac{2}{3}$ of the total depth of a candidate network, all the operations adjacent to the input nodes are of stride two. The order of ReLU-Conv-BN is kept for convolutional operations, and each separable convolution is applied twice.

DARTS [35] is adopted to search for cells and a network architecture with optimal performance. Specifically, the categorical choice of one certain operation is relaxed to a softmax over all possible operations, thus the task of cell

TABLE I
CANDIDATE OPERATORS.

| Operators | Description |
|--------------|--|
| Conv3 | Relu-Conv-Bn block with kernel size 3 |
| SpeConv3 | 3×3 separable convolutions |
| DilConv3 | 3×3 dilated separable convolution |
| MaxPoll3 | 3×3 max pooling |
| AveragePoll3 | 3×3 average pooling |
| SkipConnect | Skip connection between nodes |
| SeConnct | Squeeze-and-excitation block |
| Zero | No connections |

architecture search is reduced to learning a set of continuous variables $\alpha = \{\alpha^{(i,j)}\}$ instead of directly searching the discrete architectures, here (i, j) is the connection between node i and j and $\alpha^{(i,j)}$ means operation mixing weights for a pair of nodes (i, j) . Through this step the architecture is therefore encoded with $(\alpha_{normal}, \alpha_{reduce})$, where α_{normal} and α_{reduce} are shared by all the normal cells and reduction cells, respectively. Then all operators in O are introduced into each connection and modeled with architecture parameters. For each connection element-wise addition, referred to as mixed operation, is conducted between the outputs of each weighted operator.

To jointly learn the architecture parameter α and the weights ω within all the mixed operations, DARTS [35] treats the learning as a bi-level optimization problem, where α and ω are upper-level variable and lower-level variable, respectively. In particular, the weights ω of network is updated by minimizing training loss L_{train} while architecture parameters are fixed, and the architecture parameter α is updated by minimizing validation loss L_{val} while the weights of the network is fixed. This optimization process is expressed in Eqs. (1)&(2),

$$\alpha^* = \arg \min_{\alpha} L_{val}(\omega', \alpha), \quad (1)$$

$$\omega' = \omega - \varepsilon \nabla_{\omega} L_{train}(\omega, \alpha) \quad (2)$$

Here ε is a small value for inner optimization. α is then updated with a gradient descent method with respect to the architecture parameters,

$$\alpha = \alpha - \gamma \nabla_{\alpha}, \quad (3)$$

$$\nabla_{\alpha} = \nabla_{\alpha} L_{val}(\omega', \alpha) - \varepsilon \nabla_{\alpha, \omega}^2 L_{train}(\omega, \alpha) \nabla_{\omega'} L_{val}(\omega', \alpha), \quad (4)$$

where γ is the learning rate. It is worth mentioning that within the optimization there exists a second-order derivative, which causes expensive computational costs, thus we adopt Hessian-vector products here to approximate the second-order derivative [35], which can significantly reduce the computational complexity.

III. EXPERIMENTS

Dataset: To evaluate efficacy of the proposed methods, comparative experiments were conducted on the widely used large NTU RGB+D [38] and Kinetics [39]. As one of the largest indoor-captured datasets for human action recognition, NTU RGB+D is currently widely used. It has in total 56000

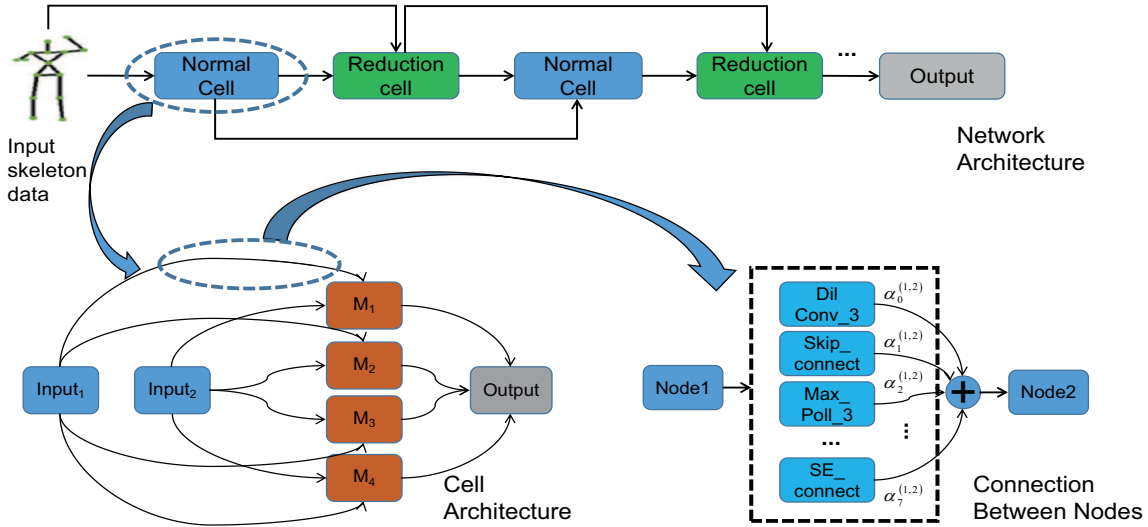


Fig. 1. Overview of the architecture searching process. The network is stacked by several cells, and each cell takes the output of two previous cells as input. In each cell there are 7 nodes including two input nodes, four intermediate nodes and one output node. On each edge, a mixture of candidate operations is placed to relax the search space.

action clips performed by 40 different actors. They are captured at different heights and horizontal angles in an indoor lab environment, with three cameras recording simultaneously. The actions cover 60 classes. Classes 1 to 49 are single-actor actions and classes 50 to 60 are actions involving two actors. The modalities of NTU RGB+D dataset include 3D skeleton, depth sequences, RGB and infrared videos. In our experiment only skeleton data were used. There are 25 joints for each subject and each joint is represented by its 3D location (X; Y; Z) in the camera coordinate system. There are two commonly used evaluation protocols:

- Cross-subject (CS) in which there are 40320 training clips and 16560 clips for evaluation. In this setting, the training parts are from a subset of actors while the evaluating parts come from the rest of actors;
- Cross-view (CV) in which there are 37920 clips for training and 18960 clips for evaluation. The training clips in this setting come from the second and third cameras and the clips captured by the first camera are for evaluation. We follow these protocols and report their top-1 recognition accuracy.

Deepmind Kinetics human action dataset [39] contains around 300,000 video clips retrieved from YouTube, which covers 400 human action classes. The estimated joint locations obtained from OpenPose toolbox are used as skeleton data. The toolbox gives 2D coordinates (X, Y) in the pixel coordinate system and confidence scores C for the 18 joints. Then each joint is represented with a tuple of (X, Y, C) and a skeleton frame is recorded as an array of 18 tuples. Two persons are selected with the highest average joint confidence in each clip for the multi-person cases. In this way, one clip

with T frames can be transformed into a skeleton sequence of these tuples. In the experiment, we use 240435 clips for training and 19796 clips for evaluation, which follows the AS-GCN [40]. The top-1 and top-5 recognition accuracy are reported.

Implementation: In the process of searching for an optimal architecture, network training and architecture update are alternatively performed. Each skeleton sequence of an action instance is preprocessed to $T = 112$ frames through uniform sampling and $N = 50$ joints in NTU RGB+D, $N = 36$ joints in Kinetics through padding with zeros if there is only one subject performing the action. The network in searching process is stacked by 6 cells including 4 identical normal cells and 2 identical reduction cells searched by the method. Both two types of cells are initialized with 16 channels and consist of 7 nodes including 2 input, 4 intermediate and 1 output nodes. We search for 35 epochs, initial learning rate is set as 0.015 and is decreased at each iteration. When a search procedure is finished, an optimal 6 cell network is returned according to the learned architecture parameters and the network is trained from scratch. In the network, two top-weighted non-zero operations are retained.

The final network is built using the searched optimal cell structures. Based on the performance on NTU RGB+D using the cross-subject protocol shown in Table II, it is found that the network stacked by 9 cells achieved the best performance. Noted that the reduction cells locate at the third and sixth layers of the network. Then the final network is trained with 350 epochs, the initial learning rate is set as 0.01 and decreased each iteration steps with a momentum of 0.9.

Results: The search was performed on a single NVIDIA

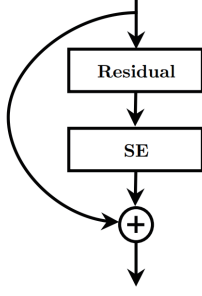


Fig. 2. Standard SE-ResNet block [37].

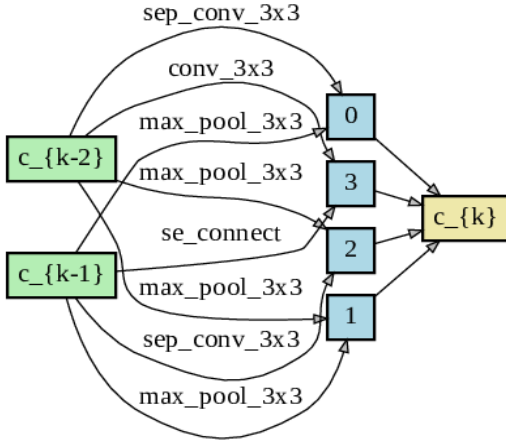


Fig. 3. Normal cell structure searched by the proposed method.

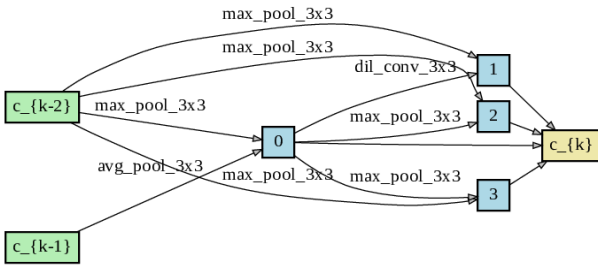


Fig. 4. Reduction cell structure searched by the proposed method.

TABLE II
PERFORMANCE COMPARISON OF FINAL NETWORK WITH DIFFERENT DEPTH OF CELLS ON THE NTU RGB+D DATASET USING CROSS-SUBJECT PROTOCOL.

| Depth of cells | Top-1 accuracy | Flops |
|----------------|----------------|-------|
| 7 | 81.2% | 8.09G |
| 8 | 84.1% | 9.09G |
| 9 | 86.4% | 10.2G |
| 10 | 85.0% | 11.1G |
| 11 | 84.8% | 12.1G |

TABLE III
PERFORMANCE COMPARISON WITH THE STATE-OF-THE-ART METHODS ON THE NTU RGB+D DATASET USING CROSS-SUBJECT AND CROSS-VIEW PROTOCOL.

| Architecture | Parameters | cross-subject | cross-view |
|------------------------|------------|---------------|------------|
| LSTM-CNN [41] | 60M+ | 82.9% | 90.1% |
| DCM (DenseNet161) [42] | 10M+ | 84.5% | 91.3% |
| DPRL + GCNN [28] | - | 83.5% | 89.8% |
| HCN [29] | 2.64M | 86.5% | 91.1% |
| ST-GCN [43] | 3.1M | 81.5% | 88.3% |
| AS-GCN [40] | 7.1M | 86.8% | 94.2% |
| DARTS [35] | 1.6M | 83.9% | 92.0% |
| SAR-NAS (Ours) | 1.3M | 86.4% | 94.3% |

TABLE IV
PERFORMANCE COMPARISON WITH THE STATE-OF-THE-ART METHODS ON THE KINETICS DATASET

| Architecture | Parameters | Top-1 accuracy | Top-5 accuracy |
|--------------------|------------|----------------|----------------|
| Temporal Conv [44] | - | 20.3% | 40.0% |
| ST-GCN [43] | 3.1M | 30.7% | 52.8% |
| AS-GCN [40] | 7.1M | 34.8% | 56.5% |
| DARTS [35] | 2.7M | 32.1% | 54.0% |
| SAR-NAS (Ours) | 2.5M | 33.6% | 56.3% |

TitanXP GPU and the total search time on the NTU RGB+D dataset is about 29 hours. Fig. 3 and Fig. 4 show the searched normal and reduction cell architectures. The final network with 9 cells is established and trained for 350 epochs. Top-1 accuracy on the NTU RGB+D dataset obtained by the 9 cell network and its comparison to the state-of-the-art results are shown in Table III. Besides, the number of parameters of different network architectures are shown in the Table as well. The results have demonstrated that the proposed method achieved superior performance with much fewer parameters than any other methods. In particular, compared with the most advanced GCN method [40] and CNN-based method [29] on cross-subject test, the number of parameters of the proposed method is decreased by 81.7% and 58.1%, respectively, which shows that the searched network architecture is much more compact. On Kinetics, recognition performances of different architectures in terms of top-1 and top-5 accuracies are compared in Table IV. The proposed method achieves competitive performance compared with the state-of-the-art. Due to the noisy skeleton data and the limitation of CNN itself to process skeleton data compared with GCN, in terms of top-1 accuracy the proposed method is slightly lower than AS-GCN. However, the number of parameters is decreased by 64.8%, which shows the high efficiency of proposed method.

TABLE V
COMPARISON OF THE RECOGNITION OF ACTIONS WITH AND WITHOUT INCLUDING THE SE MODULE AS A CANDIDATE OPERATION ON THE NTU RGB+D DATASET USING CROSS-VIEW PROTOCOL.

| Actions | Accuracy with SE | Accuracy without SE |
|--------------|------------------|---------------------|
| Drink water | 95.0% | 94.1% |
| Brush hair | 94.6% | 91.5% |
| Wipe face | 88.3% | 84.5% |
| Back pain | 89.2% | 87.0% |
| Kicking | 97.1% | 95.9% |
| Touch pocket | 95.3% | 91.1% |

Ablation study: To validate the effectiveness of the chosen operations and hence the search space, experiments are also conducted using the operations defined in [35] to search for an optimal network for the NTU RGB+D dataset using cross-subject and cross-view protocols. Table III and Table IV show the results. It is observed that the network search from the operations defined in this paper has improved the accuracy by 2.5 and 2.3 percentage points on cross-subject and cross-view tasks, respectively, and the number of parameters reduced by 0.3M.

To verify the effectiveness of the SE module, performances of two searched networks with and without the SE operation is compared, Table V shows the recognition accuracy of some representative actions. The results have demonstrated that the SE operation is useful as expected. Moreover, visually compared with the hand-designed SE-ResNet [37] architecture for image classification as shown in Fig. 2, the position of SE module of searched network architecture is different, with the hand-designed SE module placed in the end of each residual block while the searched one located in the middle of the normal cell, as shown in Fig. 3.

IV. CONCLUSION

This paper presents the first study on searching for a network architecture for skeleton-based action recognition. The results on the NTU RGB+D dataset have shown that most of the networks developed to date for skeleton-based action recognition are likely not compact and efficient. The proposed method provides an approach to searching for such a compact network that is able to achieve comparative or even better performance than the state-of-the-art methods though the searched network architecture may be dataset-dependent.

REFERENCES

- [1] P. Wang, W. Li, P. Ogunbona, J. Wan, and S. Escalera, "Rgb-d-based human motion recognition with deep learning: A survey," *Computer Vision and Image Understanding*, vol. 171, pp. 118–139, 2018.
- [2] S. Berretti, M. Daoudi, P. Turaga, and A. Basu, "Representation, analysis, and recognition of 3d humans: A survey," *ACM Transactions on Multimedia Computing, Communications, and Applications (TOMM)*, vol. 14, no. 1s, p. 16, 2018.
- [3] A. Karpathy, G. Toderici, S. Shetty, T. Leung, R. Sukthankar, and L. Fei-Fei, "Large-scale video classification with convolutional neural networks," in *Proceedings of the IEEE conference on Computer Vision and Pattern Recognition*, 2014, pp. 1725–1732.
- [4] D. Tran, L. Bourdev, R. Fergus, L. Torresani, and M. Paluri, "Learning spatiotemporal features with 3d convolutional networks," in *Proceedings of the IEEE international conference on computer vision*, 2015, pp. 4489–4497.
- [5] L. Wang, W. Li, W. Li, and L. Van Gool, "Appearance-and-relation networks for video classification," in *Proceedings of the IEEE conference on computer vision and pattern recognition*, 2018, pp. 1430–1439.
- [6] D. Tran, H. Wang, L. Torresani, J. Ray, Y. LeCun, and M. Paluri, "A closer look at spatiotemporal convolutions for action recognition," in *Proceedings of the IEEE conference on Computer Vision and Pattern Recognition*, 2018, pp. 6450–6459.
- [7] X. Wang, R. Girshick, A. Gupta, and K. He, "Non-local neural networks," in *Proceedings of the IEEE conference on computer vision and pattern recognition*, 2018, pp. 7794–7803.
- [8] C. Feichtenhofer, H. Fan, J. Malik, and K. He, "Slowfast networks for video recognition," in *Proceedings of the IEEE international conference on computer vision*, 2019, pp. 6202–6211.
- [9] K. Simonyan and A. Zisserman, "Two-stream convolutional networks for action recognition in videos," in *Advances in neural information processing systems*, 2014, pp. 568–576.
- [10] L. Wang, Y. Xiong, Z. Wang, Y. Qiao, D. Lin, X. Tang, and L. Van Gool, "Temporal segment networks: Towards good practices for deep action recognition," in *European conference on computer vision*. Springer, 2016, pp. 20–36.
- [11] C. Feichtenhofer, A. Pinz, and R. P. Wildes, "Spatiotemporal multiplier networks for video action recognition," in *Proceedings of the IEEE conference on computer vision and pattern recognition*, 2017, pp. 4768–4777.
- [12] P. Wang, W. Li, Z. Gao, J. Zhang, C. Tang, and P. O. Ogunbona, "Action recognition from depth maps using deep convolutional neural networks," *IEEE Transactions on Human-Machine Systems*, vol. 46, no. 4, pp. 498–509, 2016.
- [13] Z. Shi and T.-K. Kim, "Learning and refining of privileged information-based rnns for action recognition from depth sequences," in *Proceedings of the IEEE Conference on Computer Vision and Pattern Recognition*, 2017, pp. 3461–3470.
- [14] P. Wang, W. Li, Z. Gao, C. Tang, and P. O. Ogunbona, "Depth pooling based large-scale 3-d action recognition with convolutional neural networks," *IEEE Transactions on Multimedia*, vol. 20, no. 5, pp. 1051–1061, 2018.
- [15] M. Liu, H. Liu, and C. Chen, "3d action recognition using multiscale energy-based global ternary image," *IEEE Transactions on Circuits and Systems for Video Technology*, vol. 28, no. 8, pp. 1824–1838, 2017.
- [16] P. Wang, W. Li, Z. Gao, Y. Zhang, C. Tang, and P. Ogunbona, "Scene flow to action map: A new representation for rgb-d based action recognition with convolutional neural networks," in *Proceedings of the IEEE Conference on Computer Vision and Pattern Recognition*, 2017, pp. 595–604.
- [17] P. Wang, W. Li, J. Wan, P. Ogunbona, and X. Liu, "Cooperative training of deep aggregation networks for rgb-d action recognition," in *Thirty-Second AAAI Conference on Artificial Intelligence*, 2018.
- [18] Y. Xiao, J. Chen, Y. Wang, Z. Cao, J. T. Zhou, and X. Bai, "Action recognition for depth video using multi-view dynamic images," *Information Sciences*, vol. 480, pp. 287–304, 2019.
- [19] P. Wang, Z. Li, Y. Hou, and W. Li, "Action recognition based on joint trajectory maps using convolutional neural networks," in *Proceedings of the 24th ACM international conference on Multimedia*, 2016, pp. 102–106.
- [20] C. Li, Y. Hou, P. Wang, and W. Li, "Joint distance maps based action recognition with convolutional neural networks," *IEEE Signal Processing Letters*, vol. 24, no. 5, pp. 624–628, 2017.
- [21] Q. Ke, M. Bennamoun, S. An, F. Sohel, and F. Boussaid, "A new representation of skeleton sequences for 3d action recognition," in *Proceedings of the IEEE conference on computer vision and pattern recognition*, 2017, pp. 3288–3297.
- [22] Y. Hou, Z. Li, P. Wang, and W. Li, "Skeleton optical spectra-based action recognition using convolutional neural networks," *IEEE Transactions on Circuits and Systems for Video Technology*, vol. 28, no. 3, pp. 807–811, 2018.
- [23] Y. Du, W. Wang, and L. Wang, "Hierarchical recurrent neural network for skeleton based action recognition," in *Proceedings of the IEEE conference on computer vision and pattern recognition*, 2015, pp. 1110–1118.
- [24] H. Wang and L. Wang, "Modeling temporal dynamics and spatial configurations of actions using two-stream recurrent neural networks," in *Proceedings of the IEEE Conference on Computer Vision and Pattern Recognition*, 2017, pp. 499–508.
- [25] J. Liu, A. Shahroudy, D. Xu, A. C. Kot, and G. Wang, "Skeleton-based action recognition using spatio-temporal lstm network with trust gates," *IEEE transactions on pattern analysis and machine intelligence*, vol. 40, no. 12, pp. 3007–3021, 2018.
- [26] S. Li, W. Li, C. Cook, C. Zhu, and Y. Gao, "Independently recurrent neural network (indrn): Building a longer and deeper rnn," in *Proceedings of the IEEE Conference on Computer Vision and Pattern Recognition*, 2018, pp. 5457–5466.
- [27] C. Si, W. Chen, W. Wang, L. Wang, and T. Tan, "An attention enhanced graph convolutional lstm network for skeleton-based action recognition," in *Proceedings of the IEEE Conference on Computer Vision and Pattern Recognition*, 2019, pp. 1227–1236.
- [28] Y. Tang, Y. Tian, J. Lu, P. Li, and J. Zhou, "Deep progressive reinforcement learning for skeleton-based action recognition," in *Proceedings of the IEEE Conference on Computer Vision and Pattern Recognition*, 2018, pp. 5323–5332.
- [29] C. Li, Q. Zhong, D. Xie, and S. Pu, "Co-occurrence feature learning from skeleton data for action recognition and detection with hierarchical aggregation," in *Proceedings of the Twenty-Seventh International Joint Conference on Artificial Intelligence, IJCAI-18*, 2018, pp. 786–792.

- [30] S. Song, C. Lan, J. Xing, W. Zeng, and J. Liu, "An end-to-end spatio-temporal attention model for human action recognition from skeleton data," in *Thirty-first AAAI conference on artificial intelligence*, 2017.
- [31] T. Elsken, J. H. Metzen, and F. Hutter, "Neural architecture search: A survey," *Journal of Machine Learning Research*, vol. 20, no. 55, pp. 1–21, 2019.
- [32] B. Zoph, V. Vasudevan, J. Shlens, and Q. V. Le, "Learning transferable architectures for scalable image recognition," in *Proceedings of the IEEE conference on computer vision and pattern recognition*, 2018, pp. 8697–8710.
- [33] C. Liu, L.-C. Chen, F. Schroff, H. Adam, W. Hua, A. L. Yuille, and L. Fei-Fei, "Auto-deeplab: Hierarchical neural architecture search for semantic image segmentation," in *Proceedings of the IEEE Conference on Computer Vision and Pattern Recognition*, 2019, pp. 82–92.
- [34] G. Ghiasi, T.-Y. Lin, and Q. V. Le, "Nas-fpn: Learning scalable feature pyramid architecture for object detection," in *The IEEE Conference on Computer Vision and Pattern Recognition (CVPR)*, June 2019.
- [35] H. Liu, K. Simonyan, and Y. Yang, "DARTS: Differentiable architecture search," in *International Conference on Learning Representations*, 2019.
- [36] H. Pham, M. Guan, B. Zoph, Q. Le, and J. Dean, "Efficient neural architecture search via parameters sharing," in *Proceedings of the 35th International Conference on Machine Learning*, 2018, pp. 4095–4104.
- [37] J. Hu, L. Shen, and G. Sun, "Squeeze-and-excitation networks," in *Proceedings of the IEEE conference on computer vision and pattern recognition*, 2018, pp. 7132–7141.
- [38] A. Shahroudy, J. Liu, T.-T. Ng, and G. Wang, "Ntu rgb+ d: A large scale dataset for 3d human activity analysis," in *Proceedings of the IEEE conference on computer vision and pattern recognition*, 2016, pp. 1010–1019.
- [39] W. Kay, J. Carreira, K. Simonyan, B. Zhang, C. Hillier, S. Vijayanarasimhan, F. Viola, T. Green, T. Back, P. Natsev *et al.*, "The kinetics human action video dataset," *arXiv preprint arXiv:1705.06950*, 2017.
- [40] M. Li, S. Chen, X. Chen, Y. Zhang, Y. Wang, and Q. Tian, "Actional-structural graph convolutional networks for skeleton-based action recognition," in *Proceedings of the IEEE Conference on Computer Vision and Pattern Recognition*, 2019, pp. 3595–3603.
- [41] C. Li, P. Wang, S. Wang, Y. Hou, and W. Li, "Skeleton-based action recognition using lstm and cnn," in *2017 IEEE International Conference on Multimedia & Expo Workshops (ICMEW)*, 2017, pp. 585–590.
- [42] R. Xiao, Y. Hou, Z. Guo, C. Li, P. Wang, and W. Li, "Self-attention guided deep features for action recognition," in *2019 IEEE International Conference on Multimedia and Expo (ICME)*. IEEE, 2019, pp. 1060–1065.
- [43] S. Yan, Y. Xiong, and D. Lin, "Spatial temporal graph convolutional networks for skeleton-based action recognition," in *Thirty-Second AAAI Conference on Artificial Intelligence*, 2018.
- [44] T. S. Kim and A. Reiter, "Interpretable 3d human action analysis with temporal convolutional networks," in *2017 IEEE conference on computer vision and pattern recognition workshops (CVPRW)*, 2017, pp. 1623–1631.